General Disclaimer

One or more of the Following Statements may affect this Document

- This document has been reproduced from the best copy furnished by the organizational source. It is being released in the interest of making available as much information as possible.

- This document may contain data, which exceeds the sheet parameters. It was furnished in this condition by the organizational source and is the best copy available.

- This document may contain tone-on-tone or color graphs, charts and/or pictures, which have been reproduced in black and white.

- This document is paginated as submitted by the original source.

- Portions of this document are not fully legible due to the historical nature of some of the material. However, it is the best reproduction available from the original submission.

TRW No. 32970-6001-RU-00

PARTICLE IMPACT TESTS

FINAL REPORT

Prepared for

NASA LYNDON B. JOHNSON SPACE CENTER
Houston, Texas 77058

May 1978

Contract NAS 9-15443

TRW
DEFENSE AND SPACE SYSTEMS GROUP
ONE SPACE PARK • REDONDO BEACH, CALIFORNIA 90278

TRW No. 32970-6001-RU-00

PARTICLE IMPACT TESTS

FINAL REPORT

Prepared for

NASA LYNDON B. JOHNSON SPACE CENTER
Houston, Texas 77058

May 1978

Contract NAS 9-15443

TRW
DEFENSE AND SPACE SYSTEMS GROUP
ONE SPACE PARK • REDONDO BEACH, CALIFORNIA 90278

PARTICLE IMPACT TESTS

Final Report

TRW Document No. 32970-6001-RU-00

May 1978

Prepared for

NASA Lyndon B. Johnson Space Center
Houston, Texas 77058

CONTRACT NAS 9-15443

Prepared by

G. K. Komatsu

APPROVED: J. F. Friichtenicht
J. F. Friichtenicht

TRW
DEFENSE AND SPACE SYSTEMS GROUP

One Space Park
Redondo Beach, California 90278

CONTENTS

ILLUSTRATIONS

1. INTRODUCTION

The rocket exhaust of the Interim Upper Stage (IUS) and the Spinning Solid Upper Stage (SSUS) contains high velocity Al_2O_3 particles. These particles may impact and alter the properties of the Orbiter surfaces. The Orbiter surfaces of concern are the window glass (Corning 7940), high-temperature reusable surface insulation (HRSI) and low-temperature reusable surface insulation (LRSI). Al_2O_3 impacts were simulated by high velocity titanium diboride particles produced in the TRW Micrometeoroid Facility. Detailed analysis of the craters on the test sample surfaces will be performed at the conclusion of the Particle Impact Tests program at NASA Johnson Space Center.

2. EXPERIMENT APPARATUS

The particle impact tests were performed with the TRW Micrometeoroid Facility, suitably modified to accept the test samples. This facility electrostatically accelerates micron sized particles to high velocities (typically 1-50 km $\cdot$ sec^{-1}) and has been used extensively to simulate micrometeoroid impacts on material surfaces and micrometeoroid interactions with gaseous targets. Configuration of the numerous particle detectors and support electronics, which are a part of the facility, is determined by the specific requirements of each experiment.

A block diagram of the experiment configuration used for the present tests is given in Figure 1. The source of microparticles is a two million volt Van de Graaff generator, in which the high voltage terminal has been modified to accept microparticle charging and injection equipment.[1] Particle charging is accomplished by electrically agitating a supply of microparticles, thereby causing some to come into contact with a small tungsten electrode held at a high positive potential. Contact with the electrode causes the particle to rebound with a high positive charge and surface electric field strength of $\sim 10^9$ V $\cdot$ m^{-1}. The rebounding particle then enters the accelerator tube of the Van de Graaff generator where it is accelerated by the positive potential of the generator terminal.

The final velocity obtained as the particles exit the Van de Graaff

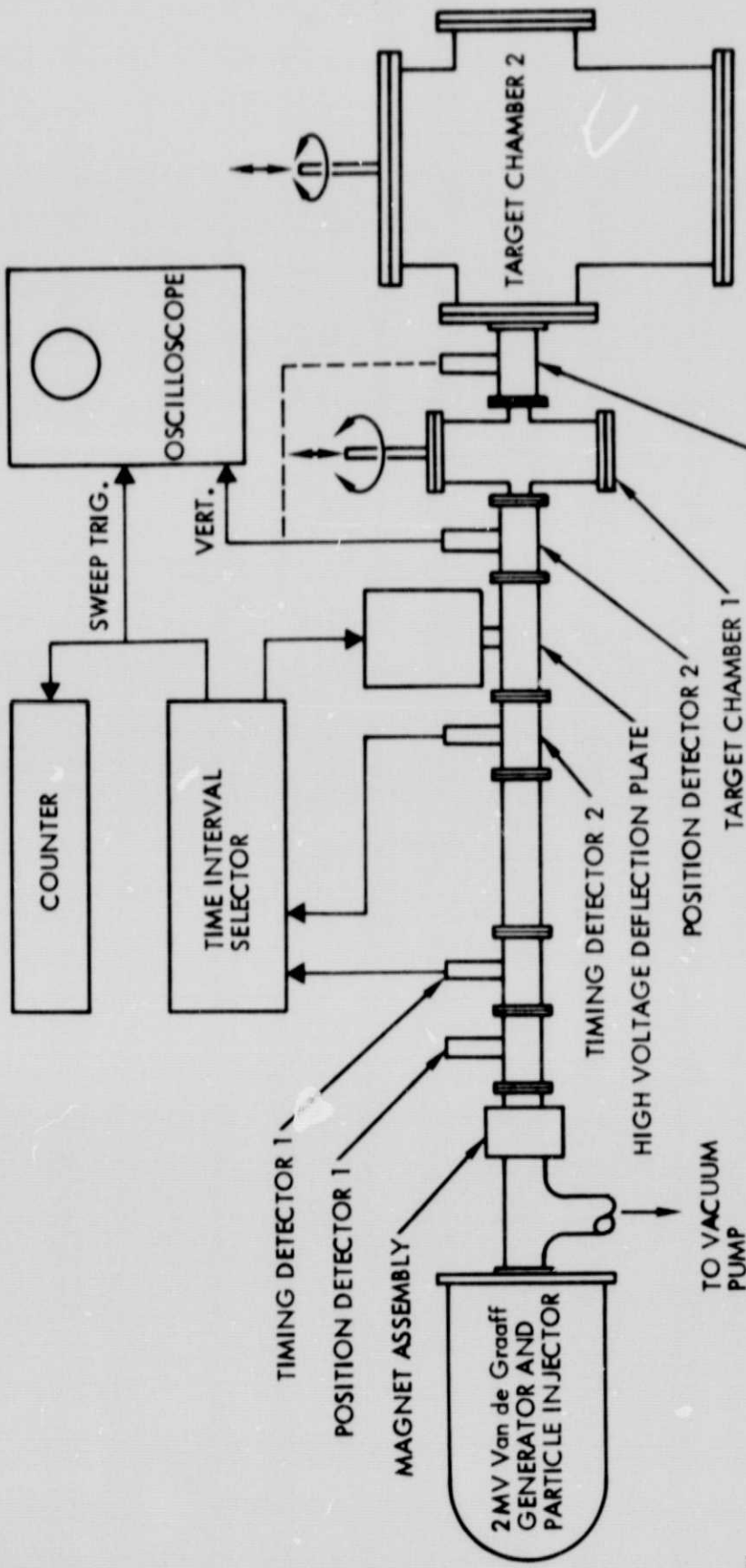

Figure 1. TRW Micrometeoroid Facility Configured for Particle Impact Tests

ORIGINAL PAGE IS
OF POOR QUALITY

generator is dependent upon the total accelerating potential, the particle material, and the particle's geometry. The upper velocity limit is dependent upon the detector electronics which are limited by signal-to-noise considerations. For most metallic materials, or materials having volume resistivities less than about 10^7 ohm-cm, the size range 0.1 to 5 microns can be accelerated to final velocities in the range from 1 to 50 km $\cdot$ sec^{-1}. The final velocity is inversely proportional to particle size with the higher velocities being obtained only with the smaller particles. Particle injection may be controlled over a wide range of output particle flux. At the lower limits it can be made essentially a single shot device while at the upper limits the output particle flux can be raised to several hundred per second.

Particles exiting from the accelerator first pass through a magnet assembly where ions, which may have been produced by the charging process, are removed. A particle position detector[2] then provides a means for locating the particle "beam" axis in order to align the system. The particles next pass through two timing detectors, separated a carefully measured distance, and the transit time over this distance is measured. The time separation of the two detector signals is analyzed by a TRW Systems Model 3212 PV2 Time Interval Selector and Dual Proportional Delay Generator.[3]

The Time Interval Selector provides an output pulse to a particle deflector when the measured transit time falls within the bounds of some predetermined time interval. Normally, with no signal applied to the input of the particle deflector high voltage electronics, all particles are deflected by a bias voltage on a pair of parallel deflector plates and are not allowed to continue downstream toward the experimental area. A signal from the Time Interval Selector removes the bias voltage for a time just sufficient to allow the selected particle to pass. The Time Interval Selector also triggers the particle counter which totals the number of velocity selected particles.

The particles pass through a second position detector, which is initially used to align the system with the particle beam axis. During an experiment, the detector output is monitored with an oscilloscope to verify that the selected particles can impact the target in the target chamber. In addition, a small sampling of the detector's output was recorded on film for analysis

later to determine particle velocity and size.

Targets to be impacted were placed in either target chamber 1 or 2, depending upon the physical size of the target. Figure 2 illustrates details of target chamber 1. Note that the holder in target chamber 1 has an aperture which can be positioned to allow particles to continue on to target chamber 2. Operation of target chamber 1 and 2 is very similar, in that the holder in both allows the sample to be moved perpendicular to the beam axis and rotated. Consequently, the impact site and impact angle can be varied without removing the sample from the chamber or letting the chamber up to atmosphere.

3. PROCEDURE

3.1 MICROPARTICLE SELECTION

Before bombarding the Orbiter materials a suitable supply of microparticles (preferred two size ranges: submicron and 2-5 micron sizes) had to be obtained. A primary requirement on the particle material was that it have a density very close to that of Al_2O_3, 3.965 g · cm^{-3}. Secondly, but just as important, the material had to be compatible with the particle charging process of the particle injector. From previous experiments, operation of the particle injector generally requires the particle material to have a bulk resistivity of < 10^7 ohm · cm. Finally, having selected candidate materials, the commercial availability of the material in the particle sizes desired was investigated.

The most promising material from the standpoint of compatibility with the particle injector was pure titanium, with a density of 4.5 g · cm^{-3}. For particle sizes < 5 microns, the material is extremely pyrophoric and, therefore, is extremely difficult to obtain. As an alternative, based upon the available data and the commercial availability, titanium dioxide (TiO_2) was obtained from Cotronics Corporation and tried in a particle injector mounted on a bench test fixture. Apparently a high bulk resistivity coupled with particle aglomeration (clump formation) in the particle reservoir resulted in an inoperative injector. Several unsuccessful schemes were attempted to reduce surface resistivity and prevent particle aglomeration. Aluminum oxide particles recovered from a rocket test were provided by

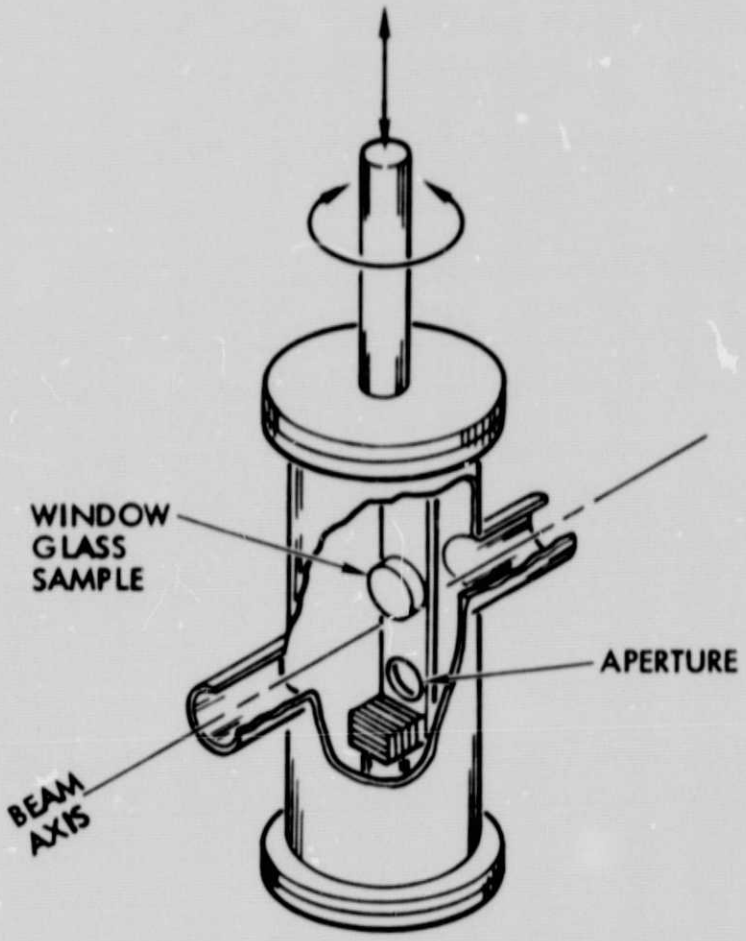

Figure 2. Isometric View of Target Chamber 1

NASA-Johnson Space Center. The bulk resistivity of this material was sufficiently large that the particle injector would not operate.

Finally, titanium diboride (TiB_2), with a density of 4.50 g · cm^{-3}, was selected and determined to function satisfactorily in the particle injector. The material was obtained from Cotronics Corporation in only the larger particle size range, 2 microns.* Particles were produced by grinding solid pieces of titanium diboride. Chiefly because this material is hard (as opposed to some solids formed as a precipitate from a chemical reaction), the supplier opted to not deliver submicron particles. Consequently, particle impact tests could not be performed with submicron particles.

3.2 TEST ARTICLES

Orbiter surfaces tested were window glass (Corning 7940), high-temperature reusable surface insulation (HRSI) and low-temperature reusable surface insulation (LRSI). The window glass samples were 1.0 in. diameter x 0.25 in. thick with a surface finish to MIL-O-13830. Twelve windows were fabricated for testing by J. L. Wood Optical Systems. Two samples each of the HRSI and LRSI were provided by NASA-Johnson Space Center with the following part numbers:

HRSI sample	1.	606020-5161
	2.	L606020-5238
LRSI sample	1.	500010-14359
	2.	L808010-500016.

Sample dimensions were 6 in. square x 2 in. thick for the HRSI and 8 in. square x 1 in. thick for the LRSI. Window glass samples were tested in target chamber 1, while HRSI and LRSI samples were tested in target chamber 2.

3.3 IMPACT SIMULATION

The Van de Graaff generator and particle injection equipment was tested and the detector array-target chamber system aligned. Particle velocity selection was exercised to exclude particles with velocities < 1 km · sec^{-1}. Impact tests were initiated on one of the glass windows to determine the

---

*Cotronics Corp. method of sizing particles is to flow a gas through a "cake" of the particles and measure the pressure drop across the "cake". Pressure drop and flow rate are then related to particle size.

required total particle deposition for a given focus condition of the particle beam from the Van de Graaff generator. These initial tests indicated a beam spot size of less than 0.12 in. (3 mm) diameter. Craters on the glass surface exhibited a great deal of spall formation with disrupted zones extending on the order of ten particle radii from the central impact site. To avoid excessive overlap of the individual craters, total particle deposition on an individual spot was held to ~ 1000 particles for the glass samples oriented such that the impact angle is 90° to the surface (see Figure 3).

The glass samples were tested wherein the impact angle was 90°, 60° and 30° to the sample surface. Total particle deposition for each angle was as follows:

1. 90° - 1030 particles
2. 60° - 1030 particles
3. 30° - 1413 particles.

Two additional cases were run at an impact angle of 90° with greater velocity selection. Particle velocities were limited to two bands, one at each extreme of the velocity range used on the previous tests. These tests, one low velocity range and one high velocity range, were performed to aid in quantifying the behavior of the surface as a function of particle size and velocity. Total particle deposition for the two cases was as follows:

1. low velocity - 142 particles
2. high velocity - 151 particles.

During the conduct of the impact tests a sampling of the position detector 2 output was recorded for later analysis.

Impact tests on the HRSI and LRSI samples followed in much the same manner as was previously described for the window glass samples. Response of both the HRSI and LRSI surfaces to the impacting particles was very similar to the glass surface; spall formation was also observed about the central impact site. Consequently, a similar rationale was employed and the total number of impacting particles for the cases of the three different impact angles was limited as indicated by the following:

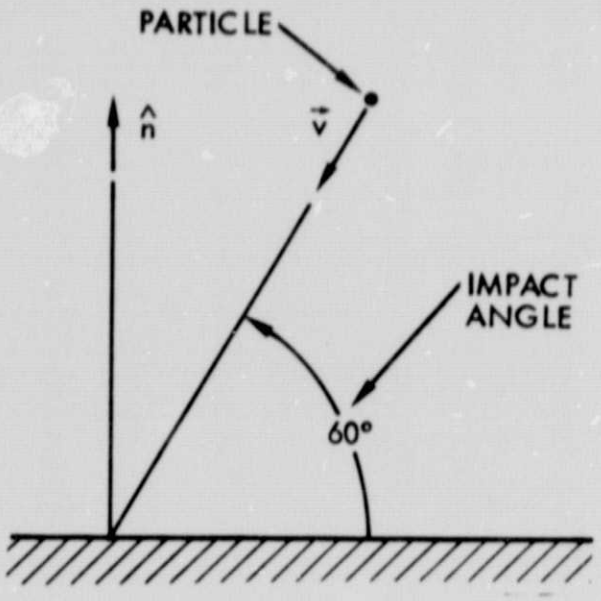

Figure 3. Impact Angle

HRSI sample (606020-5161)	1. 90°	- 1000 particles
	2. 90°	- 1017 particles
	3. 60°	- 1000 particles
	4. 30°	- 2001 particles
LRSI sample (L808010-500016)	1. 90°	- 1114 particles
	2. 90°	- 2464 particles
	3. 60°	- 1022 particles
	4. 30°	- 2025 particles.

As in the case of the glass samples, samplings of the position detector 2 output was recorded. Subsequent analysis of the position detector 2 output will be presented in Section 4.

For all three materials, impact sites were identified. Verification of the impact sites was performed utilizing a metallograph and some of the craters photographed at a magnification of 400X. These photographs will be presented in the following section.

4. RESULTS AND ANALYSIS

4.1 IMPACT SITE

The general location of the particle impact sites are known from careful measurements performed during both the set up and performance of the tests. Impact sites on the glass surfaces are readily visible with the unaided eye. However, with the HRSI and LRSI samples a metallograph was required to scan the suspected regions. Both the HRSI and the LRSI samples exhibited spall formation from the particle impacts, which greatly aided identification of the impact site. Figures 4, 5 and 6 indicate the approximate locations of the particle impacts for each of the test conditions with the three Orbiter surfaces.

4.2 CRATER PHOTOGRAPHS

Figures 7 through 14 were taken with a metallograph to illustrate crater and spall formation resulting from the impacting particles. Photographs of the glass surface at a magnification of 50X (see Figures 7A, 8A and 9A) illustrate the extent and particle distribution of the particle

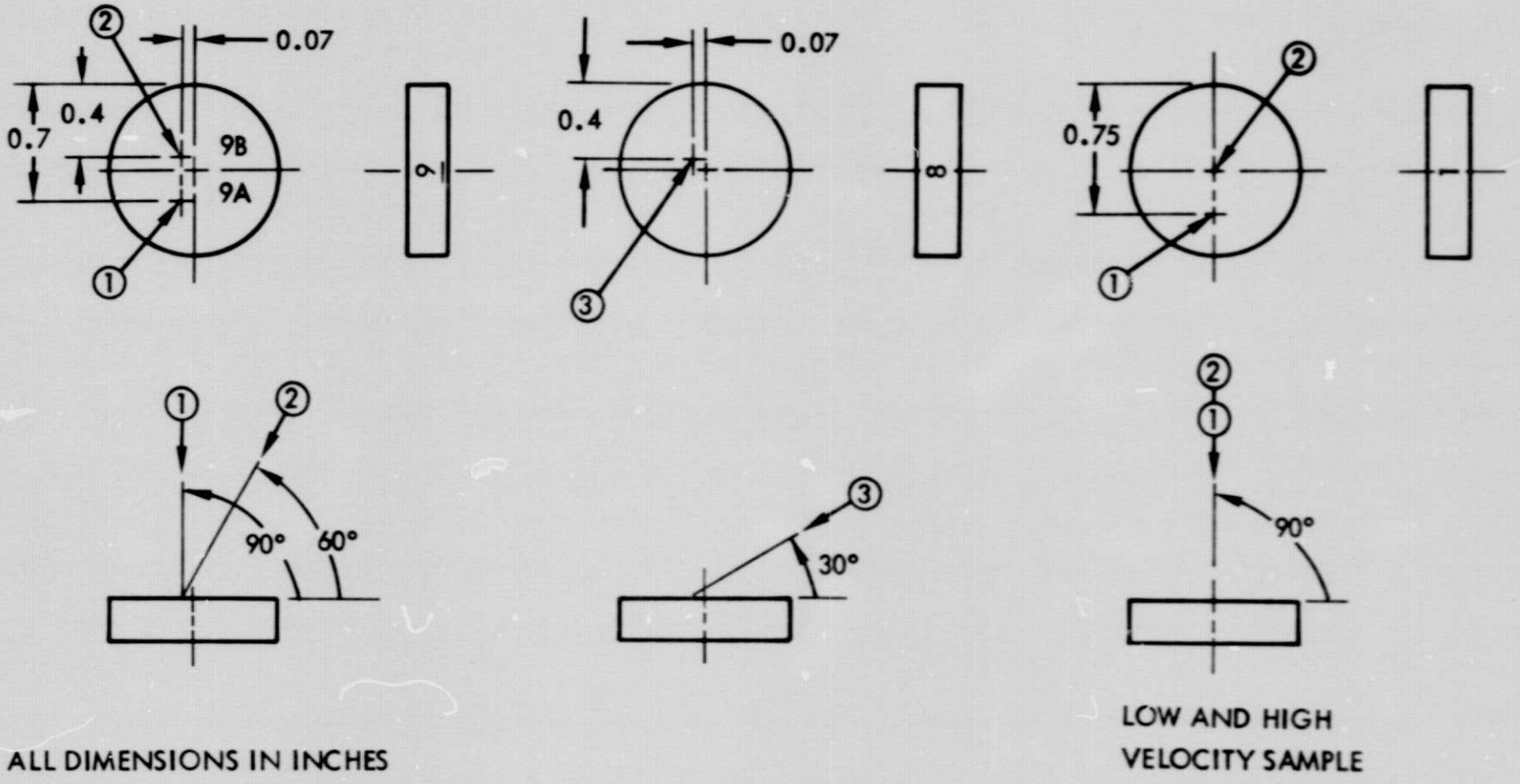

Figure 4. Window Glass Samples, Impact Site Locations

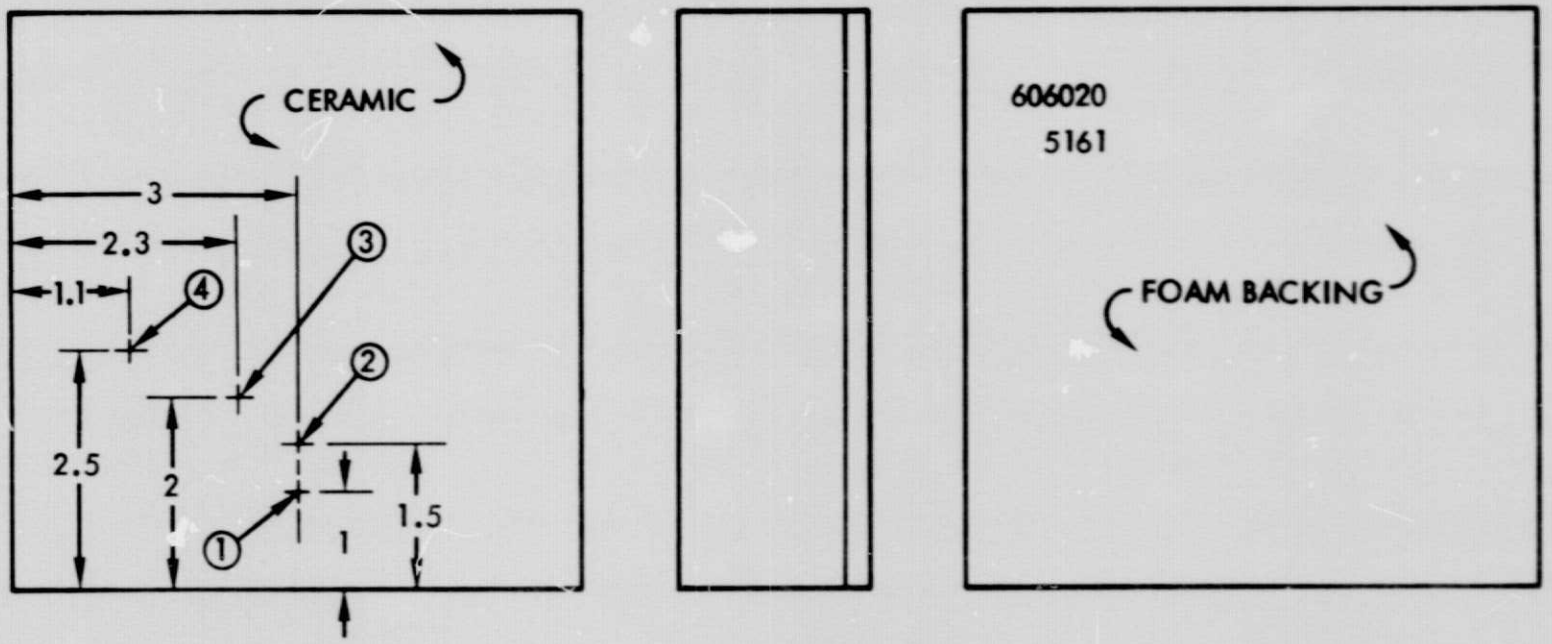

ALL DIMENSIONS IN INCHES

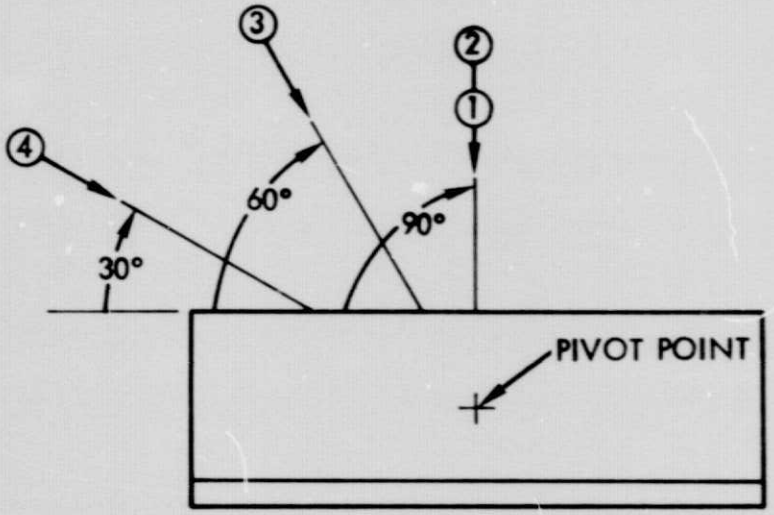

Figure 5. HRSI Sample, Impact Site Locations

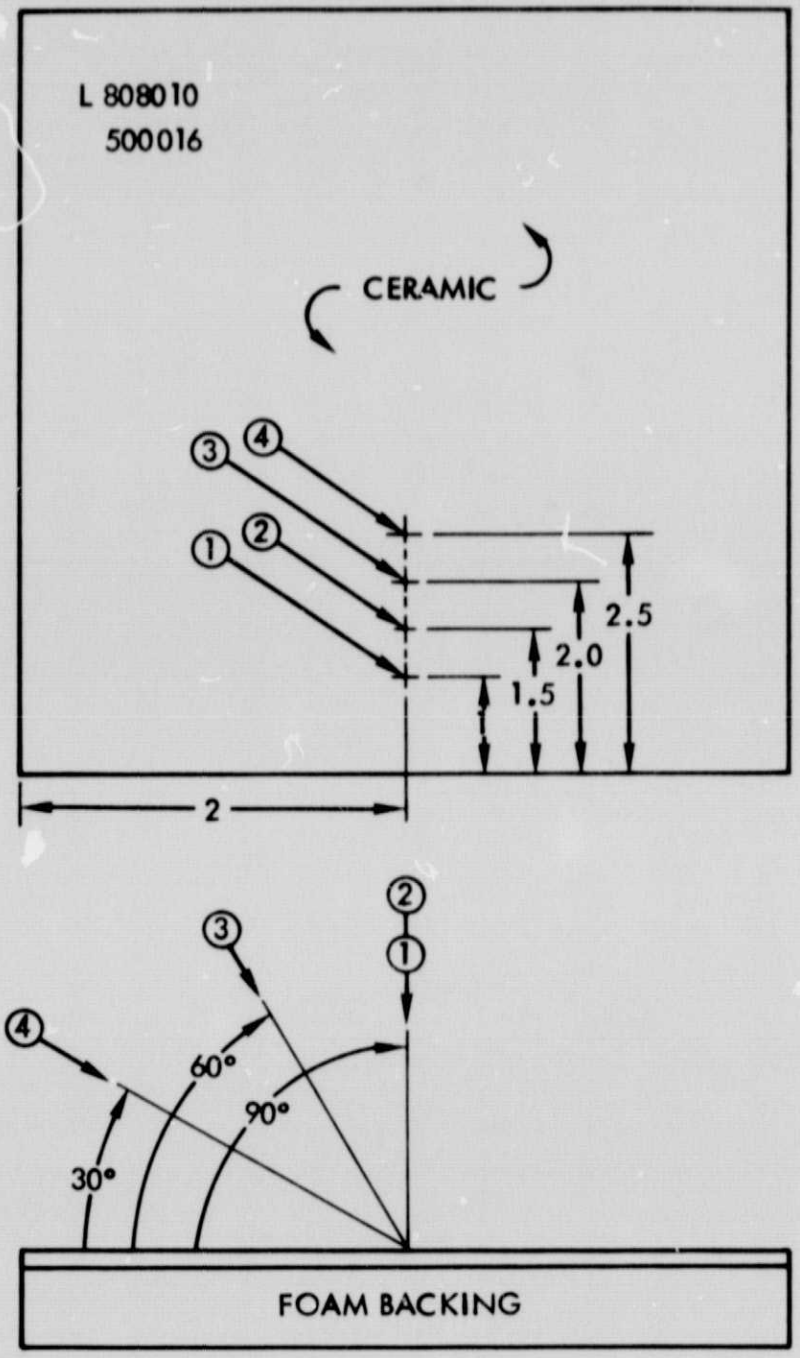

ALL DIMENSIONS IN INCHES

Figure 6. LRSI Sample, Impact Site Locations

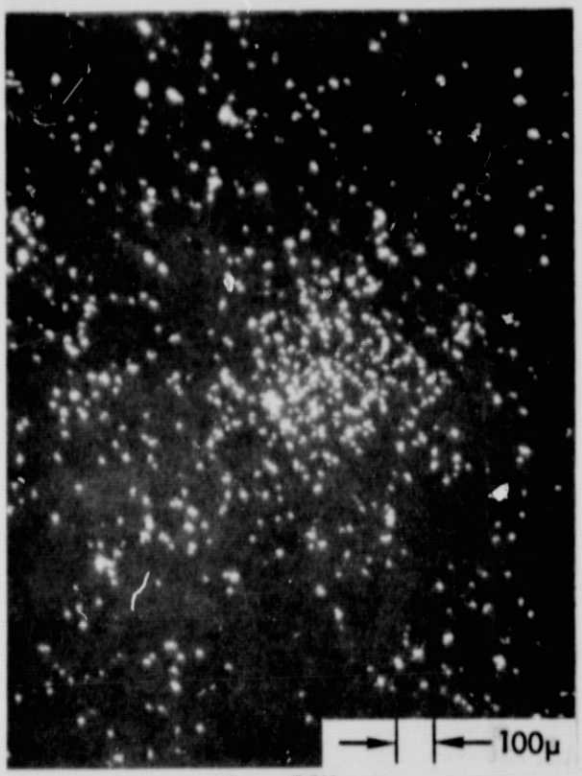

A. 50X

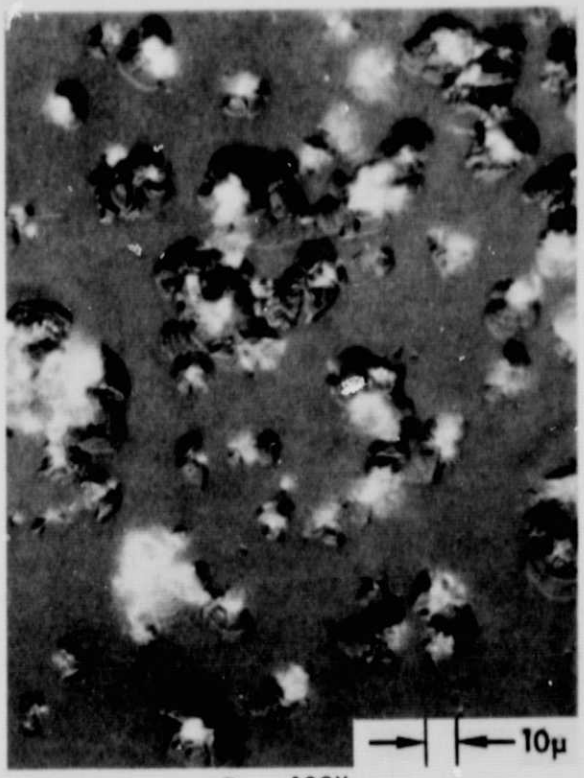

B. 400X

Figure 7. Window Glass Craters, Site 1 (90°)

A. 50X

B. 400X

Figure 8. Window Glass Craters, Site 2 (60°)

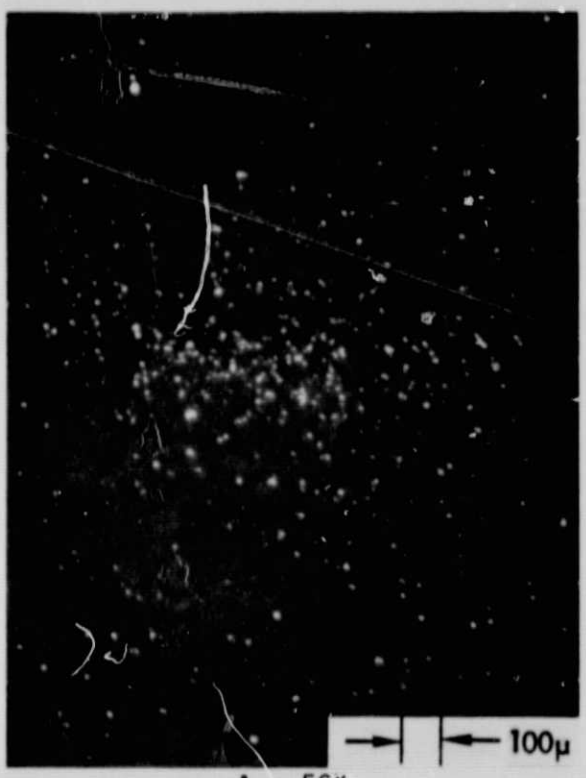

A. 50X

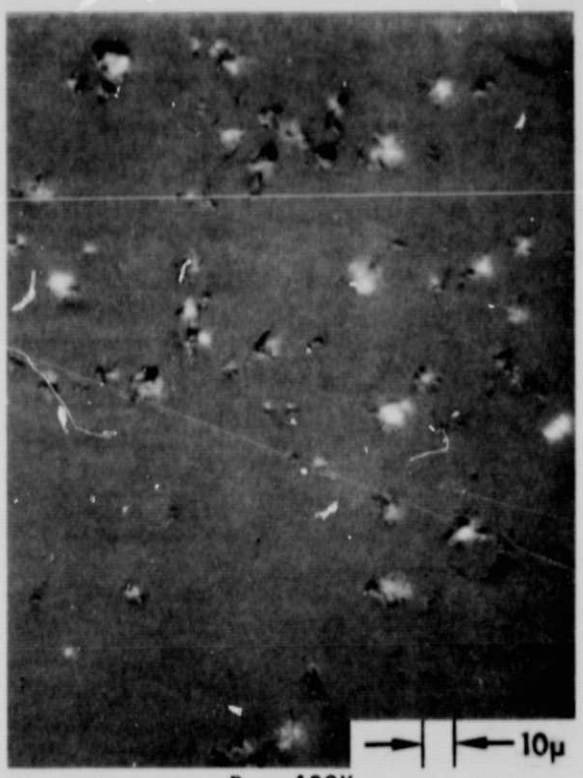

B. 400X

Figure 9. Window Glass Craters, Site 3 (30°)

Figure 10. HRSI Craters, Site 2 (90°), 400X

Figure 11. HRSI Craters, Site 3 (60°), 400X

Figure 12. HRSI Craters, Site 4 (30°), 400X

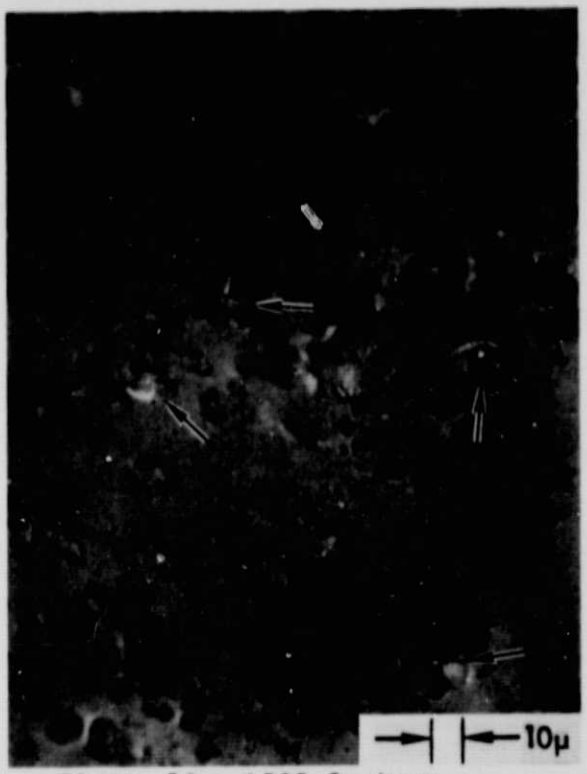

Figure 13. LRSI Craters, Site 2 (90°), 400X

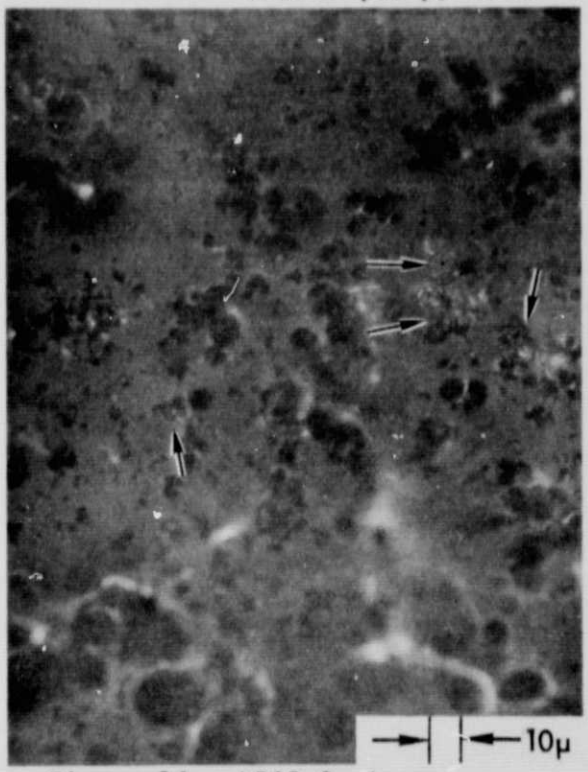

Figure 14. LRSI Craters, Site 3 (60°), 400X

beam spot. The remaining photographs were taken with a magnification of 400X. Craters on the window glass were very easy to identify. However, because of the lack of contrast, texture of the surface and limited lighting capability of the metallograph, craters on the HRSI and LRSI samples were not as well defined.

4.3 PARTICLE VELOCITY AND SIZE

Analysis of the output waveform of position detector 2 allowed calculation of particle velocity and diameter, assuming a spherical particle. The detector construction and technique for analyzing the waveform have been previously described in great detail.[4] Suffice it to say, reading the waveforms yields the particle charge, Q, and transit time, t_D, through a carefully measured portion of the detector, L_D. One can calculate the particle velocity from

$$v = \frac{L_D}{t_D} \tag{1}$$

Applying conservation of energy,

$$\frac{1}{2} mv^2 = QV \tag{2}$$

where m is the particle mass and V is the Van de Graaff terminal potential. Assuming the particle to be spherical, an effective radius of the particle is given by

$$r = \left(\frac{3QV}{2\pi\rho v^2}\right)^{1/3} \tag{3}$$

where ρ is the density of the particle material.

Particle diameters and velocities were calculated from the limited sampling of position detector output waveforms. Results of these calculations are shown in the histograms of Figures 15 through 22. The data are representative of the impacting particles for the specific Orbiter surface/impact angle case called out. From the particle size histograms, minimum particle diameter was calculated to be 4 microns. Factors which may explain the apparent size difference are the irregular shaped particles

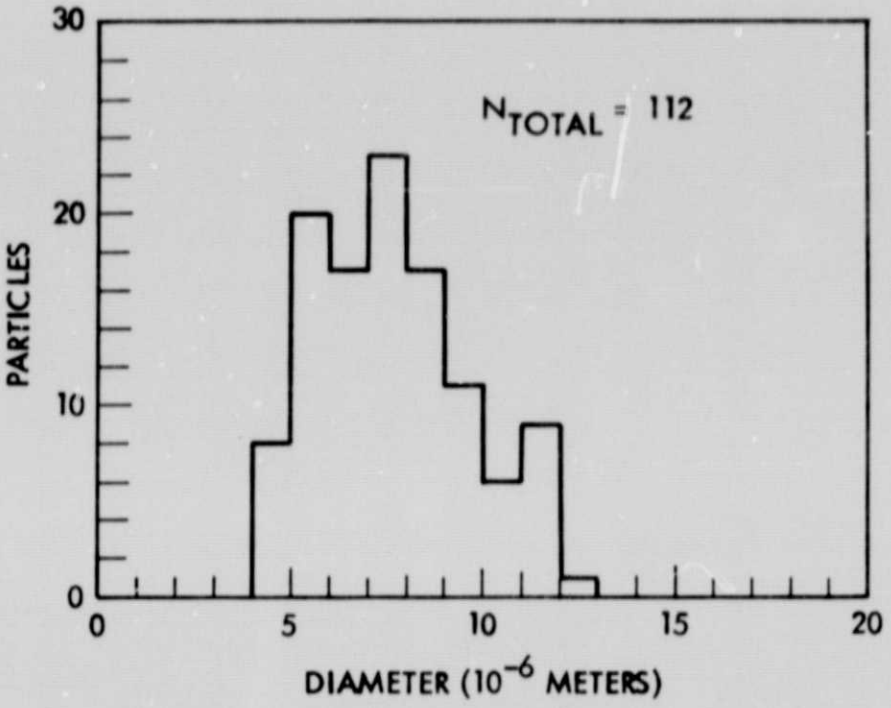

A. Particle Size Distribution

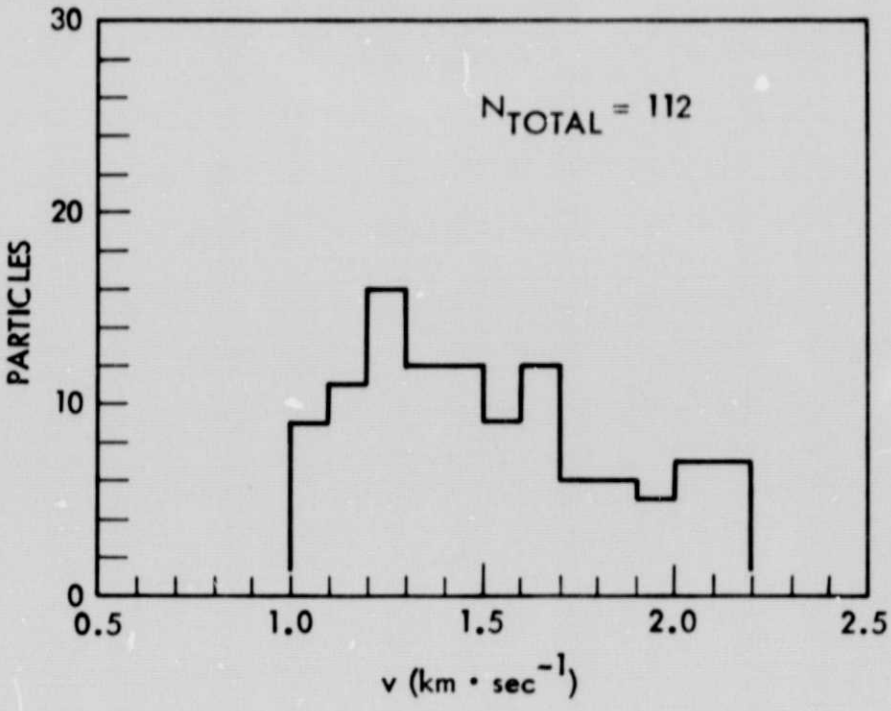

B. Particle Velocity Distribution

Figure 15. Window Glass, Sites 1 and 2

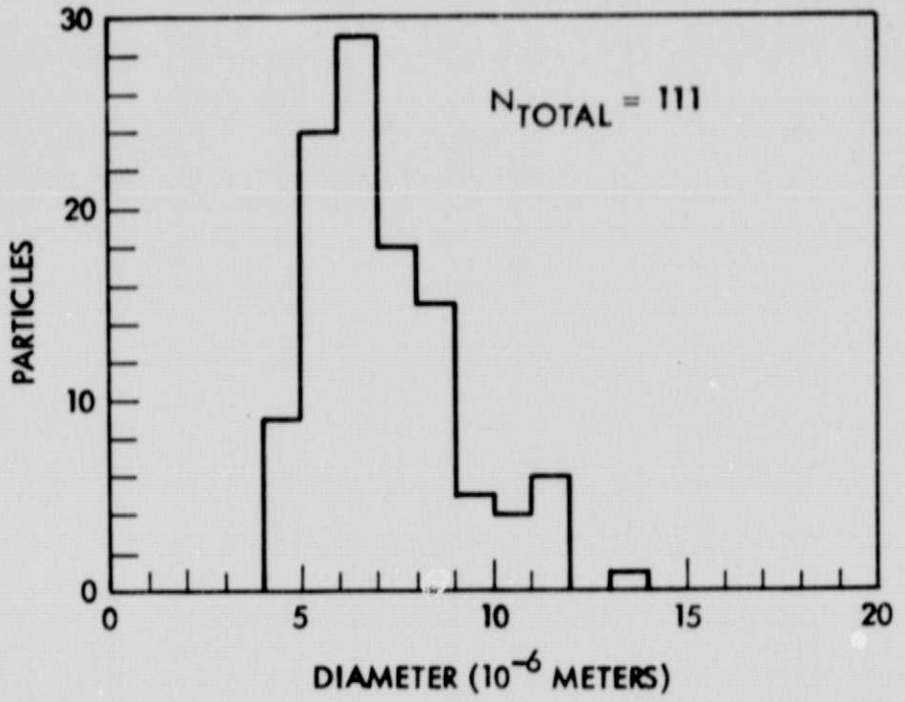

A. Particle Size Distribution

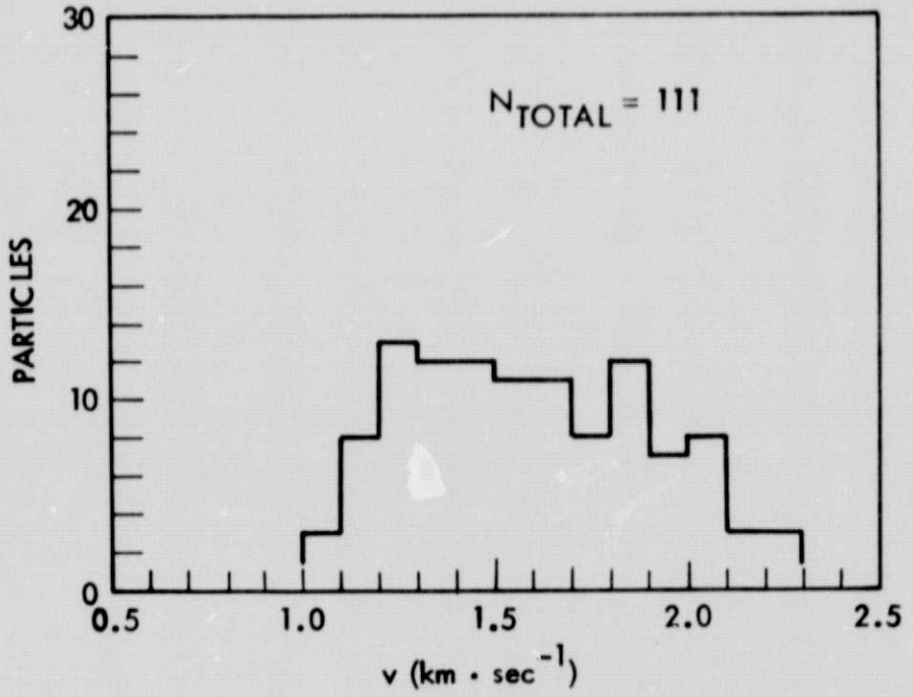

B. Particle Velocity Distribution

Figure 16. Window Glass, Site 3

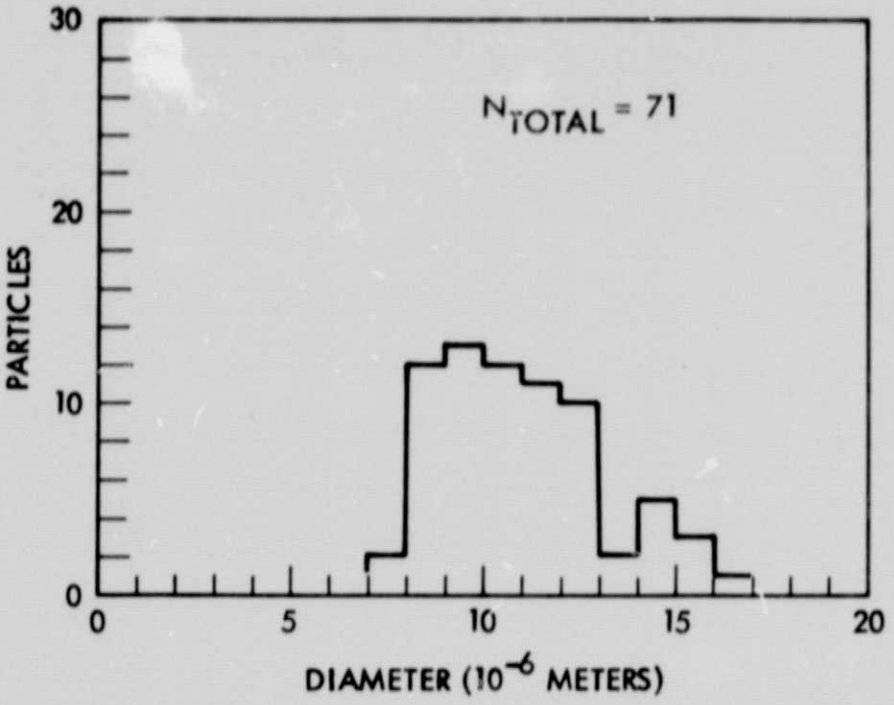

A. Particle Size Distribution

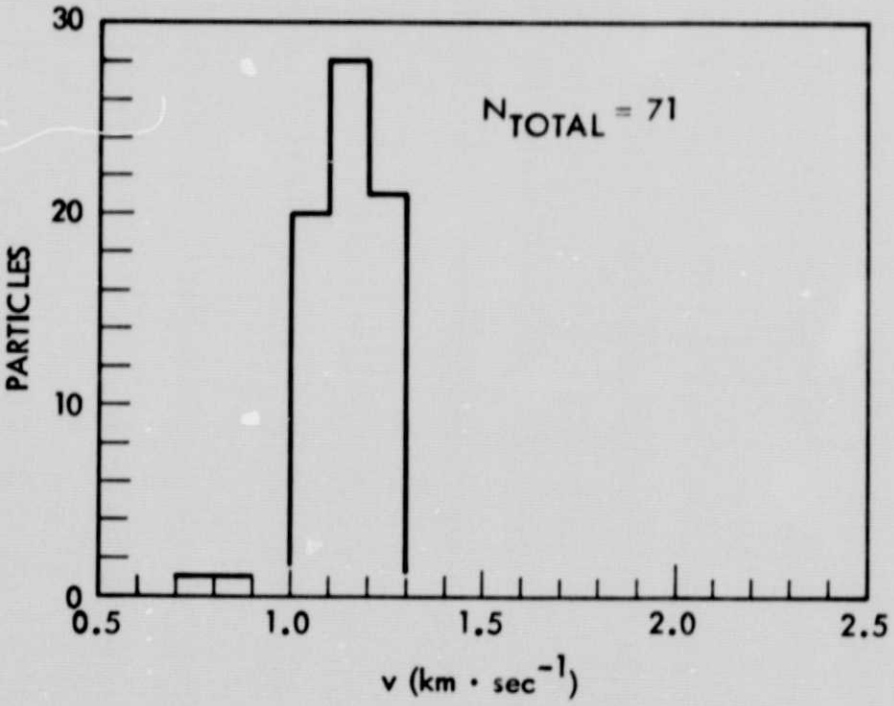

B. Particle Velocity Distribution

Figure 17. Window Glass, Low Velocity Case

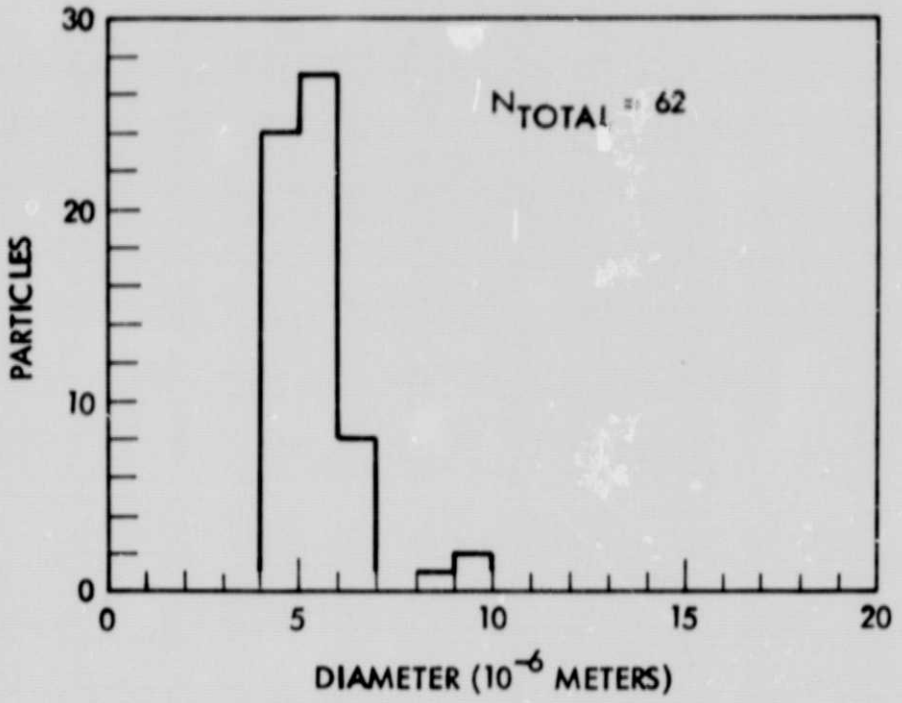

A. Particle Size Distribution

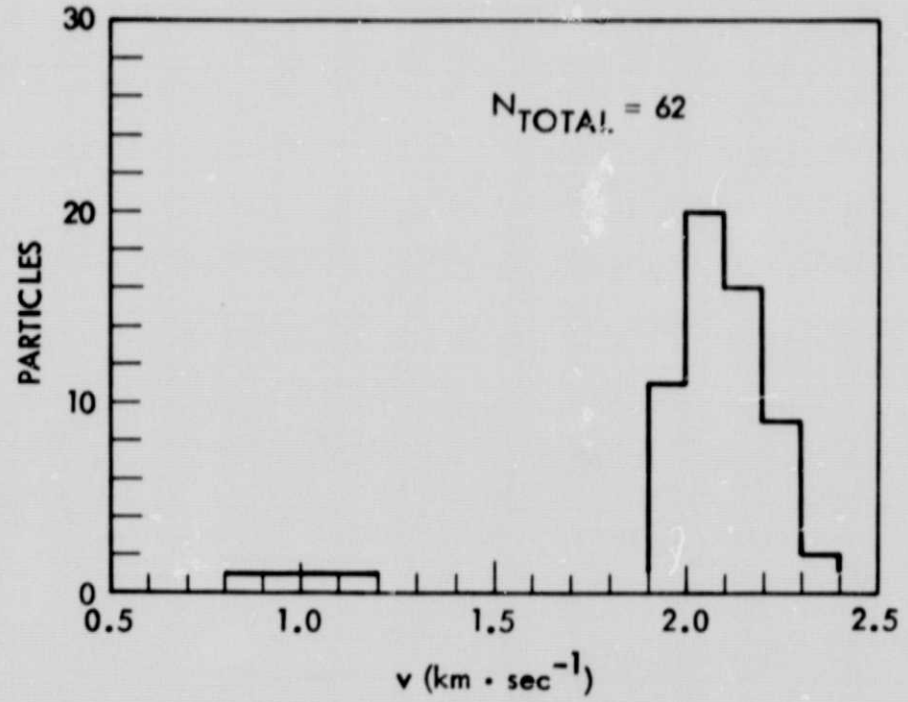

B. Particle Velocity Distribution

Figure 18. Window Glass, High Velocity Case

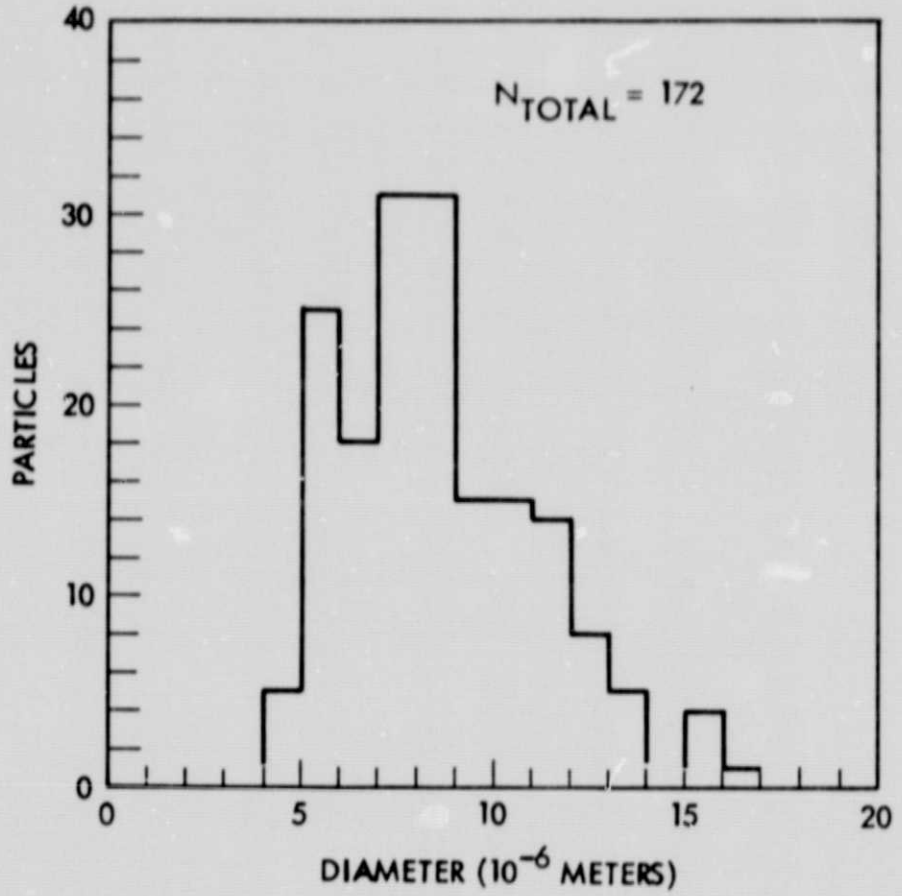

A. Particle Size Distribution

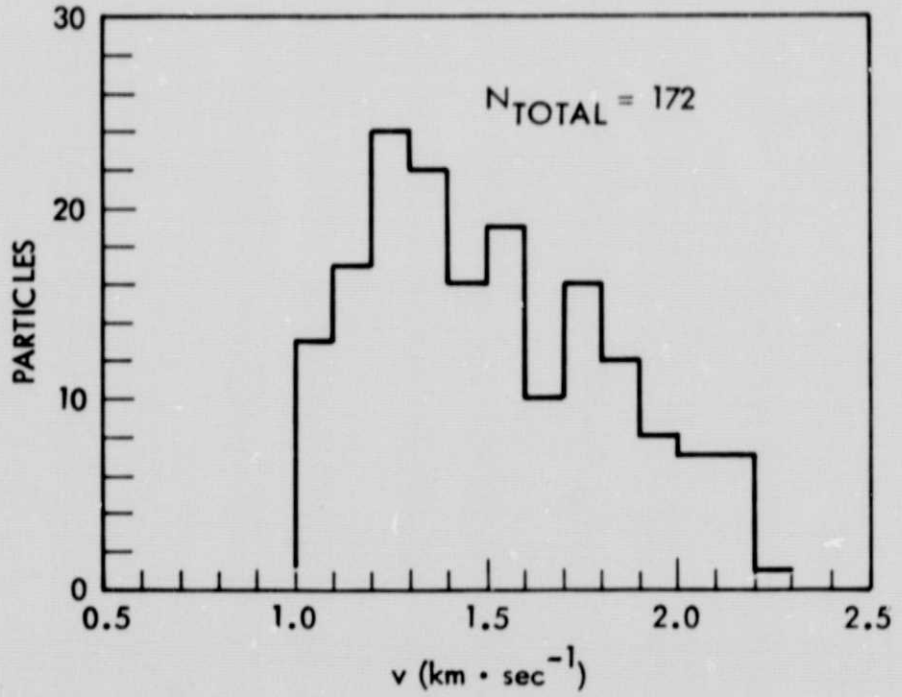

B. Particle Velocity Distribution

Figure 19. HRSI, Sites 1 and 2

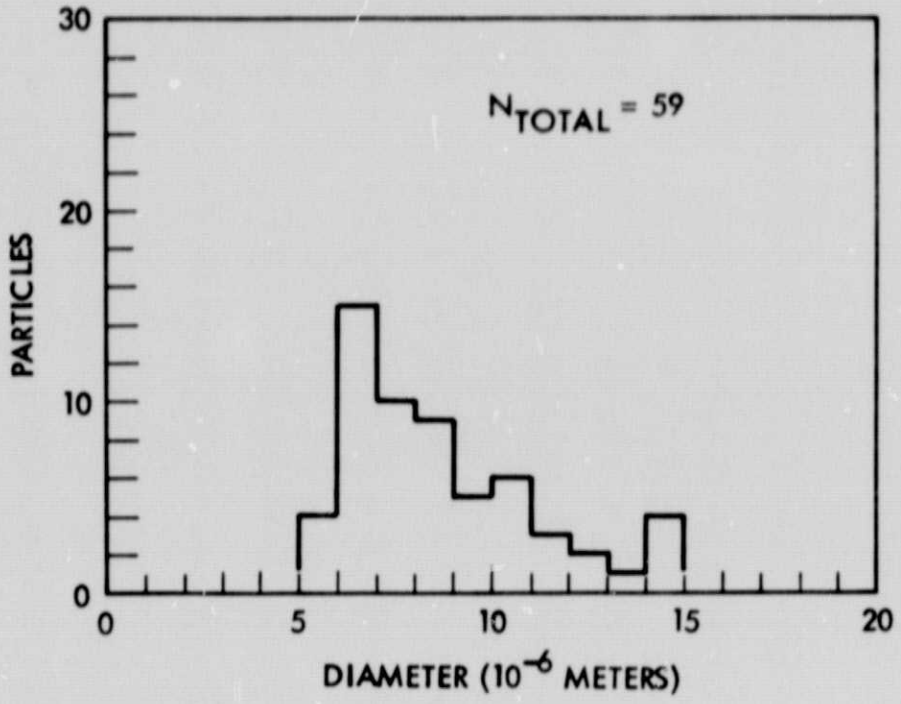

A. Particle Size Distribution

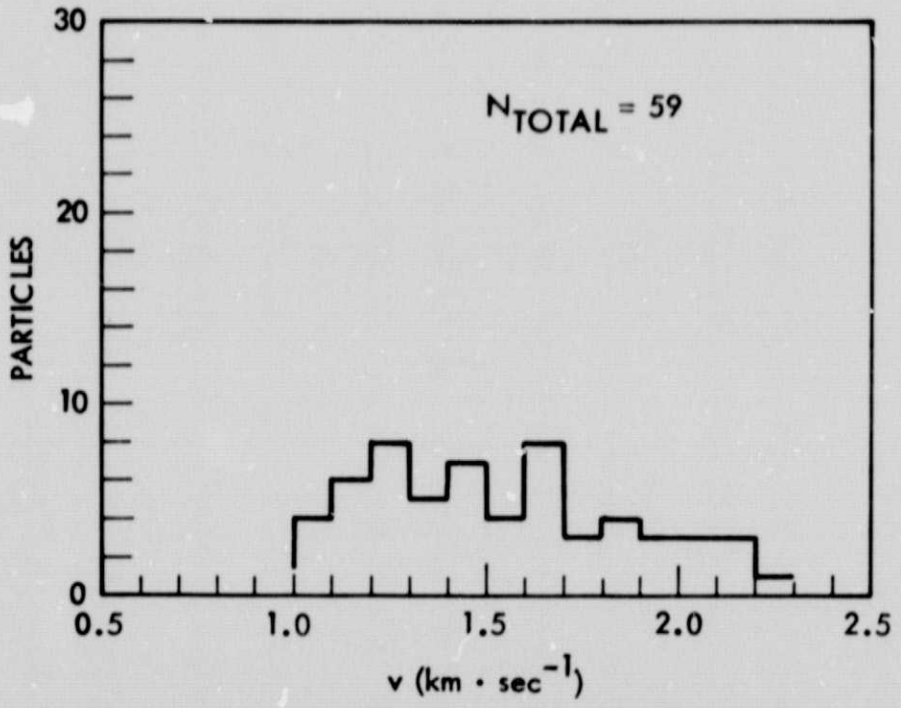

B. Particle Velocity Distribution

Figure 20. HRSI, Sites 3 and 4

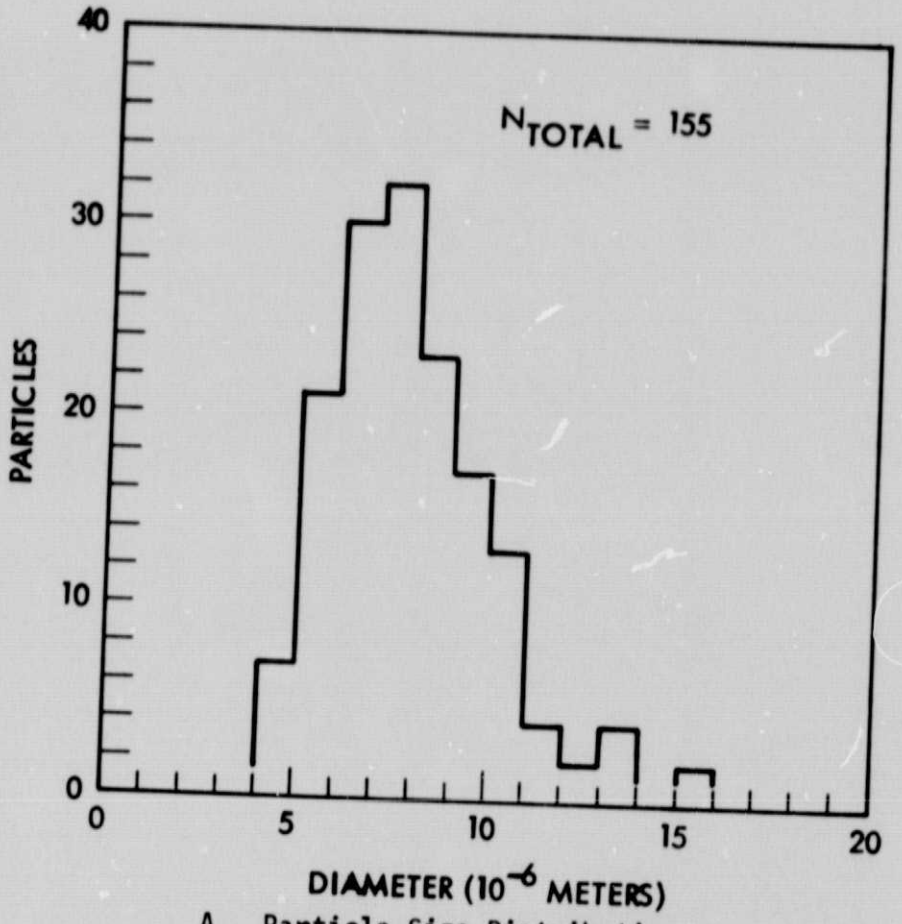

A. Particle Size Distribution

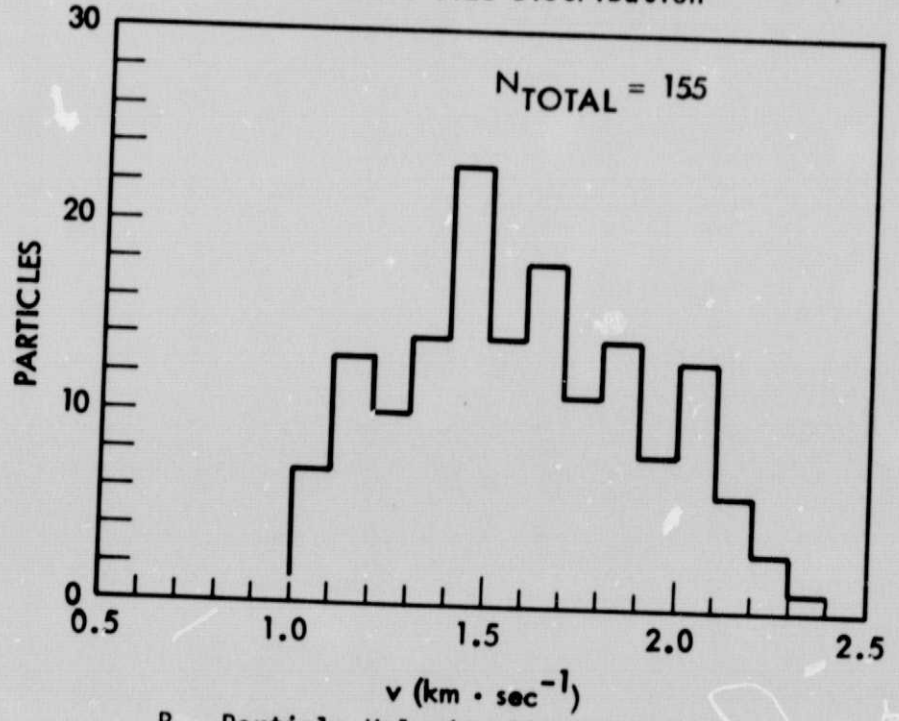

B. Particle Velocity Distribution

Figure 21. LRSI, Sites 1 and 2

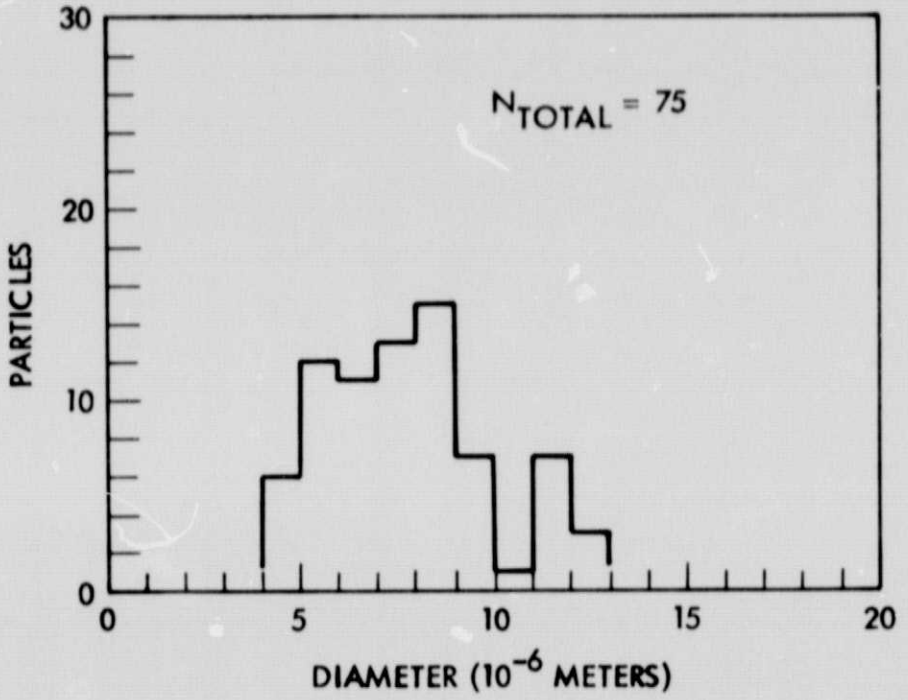

A. Particle Size Distribution

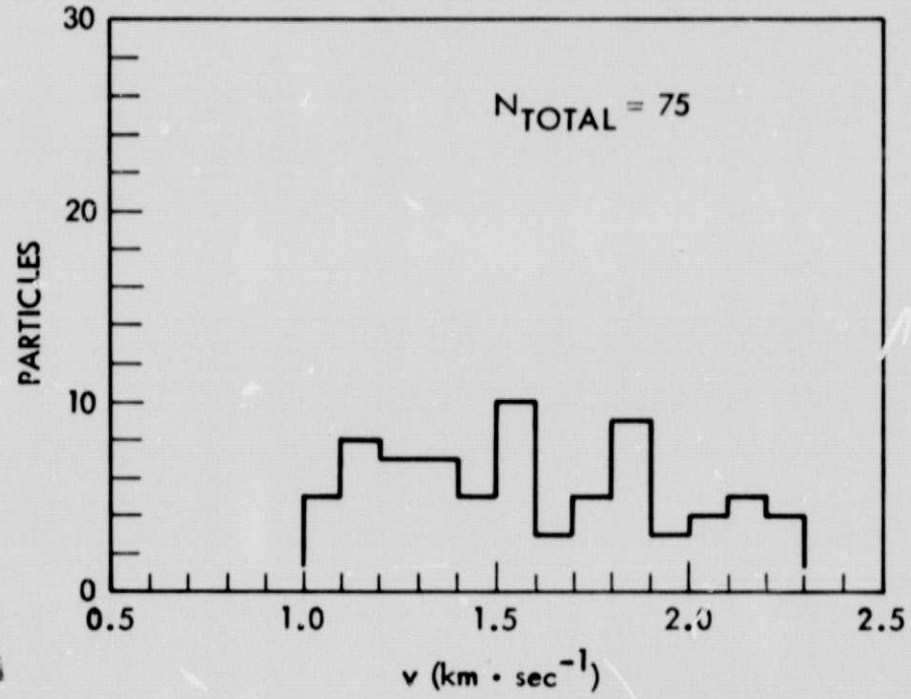

B. Particle Velocity Distribution

Figure 22. LRSI, Sites 3 and 4

produced by a grinding process and a sizing technique which may be particle geometry dependent. Also, Figures 17B and 18B indicate that very slow particles were leaking through the particle deflection system. Obviously these particles do not possess a sufficient charge-to-mass ratio to be deflected off the beam axis. It is believed that these particles have lost some of their charge, possibly through collisions with the internal structure of the particle detectors.

5. SUMMARY

Particle impact tests were performed on three types of Orbiter surface with the TRW Micrometeoroid Facility. The tests simulated the impact of Al_2O_3 particles contained in the rocket exhaust of the Interim Upper Stage and the Solid Spinning Upper Stage. Test particles were titanium diboride with typical particle velocities in the range 1-2.3 km $\cdot$ sec^{-1} and equivalent particle diameters in the range 4-16 microns. Impact angles to the material surface were 90°, 60° and 30°. The particle impact sites were located on the sample surfaces and craters were photographed with a magnification of 400X. Test surfaces will then be sent to NASA Johnson Space Center for further analysis.

REFERENCES

1. Friichtenicht, J. F., "Two-Million-Volt Electrostatic Accelerator for Hypervelocity Research," Rev. Sci. Instr., Vol. 33, No. 2, pp. 209-212, February 1962.

2. Shelton, H., Hendricks, C. D., and Wuerker, R. F., "Electrostatic Acceleration of Microparticles to Hypervelocities," J. Appl. Phys., Vol. 31, No. 7, pp. 1243-1246, July 1960.

3. Roy, N. L., and Becker, D. G., "A Time Interval Selector and Proportional Delay Generator," Rev. Sci. Instr., Vol. 42, No. 2, pp. 204-209, February 1971.

4. Operating and Service Manual: "Van de Graaff Accelerator Microparticle Modification Kit," MD-MAN-1, TRW Systems Group No. 3212-84.